SUPPORTING INFORMATION

High Ionicity Ionic Liquids (HIILs): Comparing Ethylsulfonate and Ethylsulfate Anion Effect.

Filipe S. Oliveira[a], Ana B. Pereiro[a], João M. M. Araújo[a], Carlos E. S. Bernardes[b], José N. Canongia Lopes[a,b], Smilja Todorovic[a], Gabriel Feio[c], Pedro L. Almeida[c,d], Luís P. N. Rebelo[a] and Isabel M. Marrucho[a,e*]

[a] *Instituto de Tecnologia Química e Biológica, Universidade Nova de Lisboa, Av. da República, 2780-157 Oeiras, Portugal.*
[b] *Centro de Química Estrutural, IST/UTL, 1049-001 Lisboa, Portugal*
[c] *CENIMAT/I3N, Departamento de Ciência dos Materiais, Faculdade de Ciências e Tecnologia, Universidade Nova de Lisboa, 2829-516 Caparica, Portugal*
[d] *Área Departamental de Física, Instituto Superior de Engenharia de Lisboa, R. Conselheiro Emídio Navarro, 1, 1950-062 Lisboa, Portugal*
[e] *Departamento de Química, Universidade de Aveiro, Campus Universitário de Santiago, 3810-193 Aveiro, Portugal*

*Corresponding Author: imarrucho@itqb.unl.pt (Isabel M. Marrucho)

1. Experimental Methods

1.1. Refractive index measurements

The refractive indexes were measured in the temperature range between 298.15 and 323.15 K at the sodium D-line using a Carl Zeiss Abbé refractometer with a precision of ± 5 × 10^{-5}. The temperature in the refractometer cell was controlled using an external thermostatic bath and measured with the refractometer thermometer (± 0.05 K accuracy). Samples were directly introduced in the cell (prism assembly) using a syringe.

At least three independent measurements were taken for each sample at each temperature to assure the effectiveness of the measurement. The absolute uncertainty of the refractive indices is ± 0.00005.

1.2. Thermal stability measurements

Thermogravimetric analyses (TGA) were carried out using a TA instrument Model TGA Q50. Nitrogen was used as the sample gas for the TGA measurements at a flow rate of 60 ml × min^{-1}. All samples were recorded in aluminium pans within a nitrogen atmosphere. Samples were heated to 873 K at a rate of 10 $Kmin^{-1}$ until complete thermal degradation was achieved. Universal Analysis, version 4.4A software, was used to determine the onset temperatures (T_{onset}) corresponding to the temperature at which the baseline slope changed during heating. The relative uncertainty of the

temperature is ± 0.50 %. At least three independent measurements were taken for each sample to ensure the accuracy of the measurement.

2. Results and Discussion

2.1. Ionicity

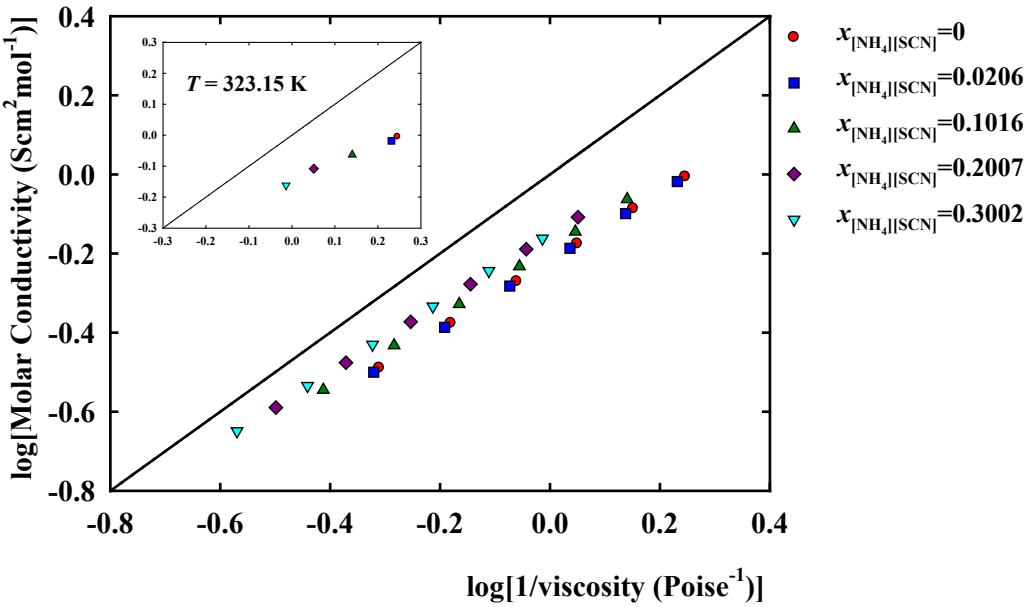

Figure S1. Walden plot for the binary system $[C_2MIM][C_2SO_3]$ + $[NH_4][SCN]$ as a function of the inorganic salt concentration. The inside figure shows the behaviour of the binary system at 323.15 K.

2.2. Density

The density values measured for the $[C_2MIM][C_2SO_3]$ + $[NH_4][SCN]$ system at temperatures between 293.15 and 323.15 K and at atmospheric pressure are listed in Table S1. Figure S2 illustrates the temperature dependence of the density for this mixture at a concentration of 0.3 in molar fraction of $[NH_4][SCN]$ and compares it with the pure ionic liquid, $[C_2MIM][C_2SO_3]$. Also, results for the pure $[C_2MIM][C_2SO_4]$ IL and its binary mixture $[C_2MIM][C_2SO_4]$ + $[NH_4][SCN]$ (also at a IS's molar fraction of 0.3 $[NH_4][SCN]$) are plotted [S1]. The inorganic salts mole fraction of 0.3 was chosen for comparison of the two ionic liquids. The density of pure $[C_2MIM][C_2SO_4]$ is higher than the pure $[C_2MIM][C_2SO_3]$ and for both binary mixtures the density is lower than the neat ILs. This behaviour is different than that found for other binary mixtures of IL+IS where the addition of salt increased the density of the mixture. The 1-ethyl-3-methylimidazolium acetate + ammonium thiocyanate system in our previous work [S1] as

well as the mixtures of 1-ethyl-3-methylimidazolium bis(fluorosulfonyl)amide and 1-ethyl-3-methylimidazolium bis(trifluoromethylsulfonyl)amide with their respective lithium salts [S2] are examples of increased density with the addition of inorganic salt. Lassègues et al. [S3] and Monteiro et al. [S4] also reported density data of mixtures of different ILs based on alkyl-substituted imidazolium cations and bis(trifluoromethylsulfonyl)amide anions, with the lithium bis(trifluoromethylsulfonyl)amide salt, where the density of the mixture was higher than the neat IL. Moreover, the effect of the addition of $[NH_4][SCN]$ is more pronounced in the density of the $[C_2MIM][C_2SO_4]$ than the $[C_2MIM][C_2SO_3]$. This finding is corroborated by Raman data, which indicate a formation of ´unengaged´ SCN only in the former IL.

Table S1. Density, ρ, dynamic viscosity, η, ionic conductivity, σ, refractive index, n_D, molar volume, V_m, molar refraction, R_m, and free molar volume, f_m, for the binary system $[C_2MIM][C_2SO_3]$ (1) + $[NH_4][SCN]$ (2) at several temperatures.

x_2	ρ (g·cm^{-3})	η (mPa·s)	σ (mS·cm^{-1})	n_D	V_m	R_m	f_m
			T = 298.15 K				
0	1.2037	204.35	1.770	1.49181	183.0130	53.0779	129.9351
0.0206	1.2035	209.26	1.751	1.49181	180.5757	52.3711	128.2047
0.1016	1.2025	258.52	1.668	1.49482	171.0051	49.8531	121.1520
0.2007	1.2004	315.24	1.615	1.49816	159.4072	46.7385	112.6687
0.3002	1.1973	371.13	1.518	1.50184	147.8392	43.6178	104.2214
			T = 303.15 K				
0	1.2004	151.41	2.290	1.48947	183.5162	53.0084	130.5078
0.0206	1.2002	155.49	2.267	1.48947	181.0672	52.3010	128.7662
0.1016	1.1993	192.11	2.155	1.49314	171.4662	49.8436	121.6225
0.2007	1.1972	235.08	2.090	1.49615	159.8333	46.7030	113.1303
0.3002	1.1941	276.11	1.970	1.50051	148.2312	43.6348	104.5964
			T = 308.15 K				
0	1.1971	114.96	2.912	1.48846	184.0118	53.0582	130.9536
0.0206	1.1970	118.33	2.876	1.48879	181.5563	52.3806	129.1757
0.1016	1.1961	146.23	2.734	1.49248	171.9201	49.9185	122.0016
0.2007	1.1941	179.27	2.645	1.49482	160.2483	46.7172	113.5311
0.3002	1.1910	210.28	2.499	1.49917	148.6170	43.6492	104.9679
			T = 313.15 K				
0	1.1939	89.18	3.619	1.48779	184.5102	53.1401	131.3701
0.0206	1.1938	91.97	3.572	1.48846	182.0430	52.4905	129.5525
0.1016	1.1930	113.64	3.396	1.49080	172.3765	49.9061	122.4704
0.2007	1.1910	139.49	3.286	1.49448	160.6609	46.8104	113.8505
0.3002	1.1880	163.36	3.112	1.49750	148.9923	43.6353	105.3571
			T = 318.15 K				
0	1.1907	70.52	4.425	1.48545	185.0112	53.0662	131.9450
0.0206	1.1906	72.85	4.362	1.48645	182.5323	52.4474	130.0849
0.1016	1.1899	89.94	4.145	1.48980	172.8256	49.9493	122.8762
0.2007	1.1880	110.48	4.016	1.49314	161.0756	46.8235	114.2521
0.3002	1.1851	129.19	3.816	1.49716	149.3653	43.7194	105.6459
			T = 323.15 K				
0	1.1875	56.73	5.315	1.48478	185.5098	53.1469	132.3629
0.0206	1.1874	58.68	5.240	1.48511	183.0191	52.4640	130.5550
0.1016	1.1868	72.38	4.992	1.48913	173.2770	50.0212	123.2558
0.2007	1.1850	88.92	4.827	1.49248	161.4834	46.8881	114.5953
0.3002	1.1824	103.20	4.600	1.49649	149.7064	43.7689	105.9375

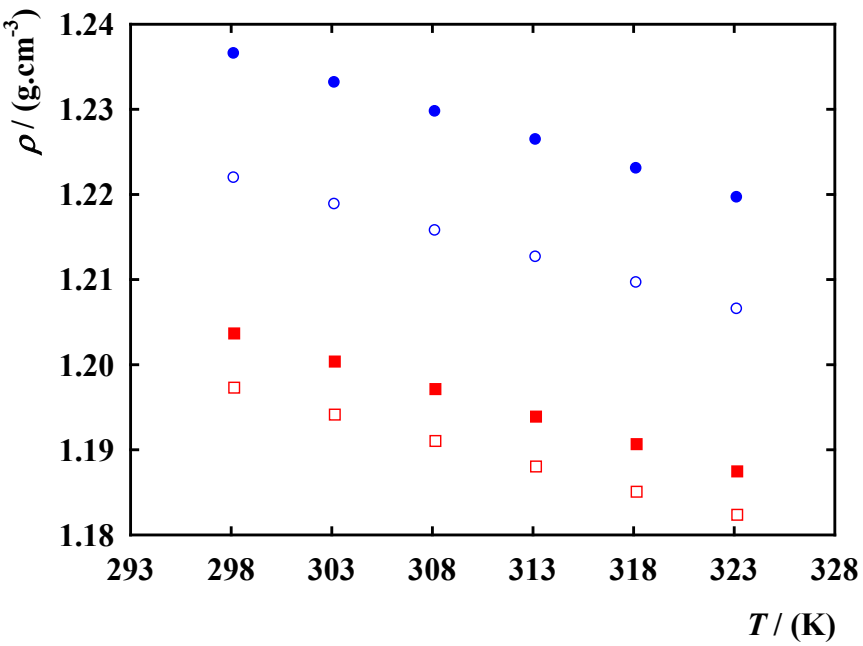

Figure S2. Density as a function of temperature for $[C_2MIM][C_2SO_4]$ [S1] (blue filled circle), $[C_2MIM][C_2SO_4]$ + $x_{[NH4][SCN]}$=0.3 [S1] (blue empty circle), $[C_2MIM][C_2SO_3]$ (red filled square) and $[C_2MIM][C_2SO_3]$ + $x_{[NH4][SCN]}$=0.3 (red empty square).

2.3. Refractive Index

The refractive indexes for the system $[C_2MIM][C_2SO_3]$ + $[NH_4][SCN]$ are shown in Table S1, for the concentration range between 0 and 0.3 mole fraction of salt. For the system $[C_2MIM][C_2SO_4]$ + $[NH_4][SCN]$, the refractive indexes along with the molar volume, molar refraction, and free molar volume values are depicted in Table S2 for the all concentration range of salt. In both systems, the addition of salt increased the refractive index of the mixture, and within the studied concentration range of $[NH_4][SCN]$, it decreased linearly with increasing temperature.

The Lorentz–Lorenz equation (1) can be used to calculate the molar refraction or molar polarizability [S5], R_m, which can be related both to density, ρ, and refractive index, n_D.

$$R_m = \left(\frac{n_D^2 - 1}{n_D^2 + 2}\right) V_m \qquad (1)$$

where V_m is the molar volume. The molar refraction is considered as a measure of the hard-core volume of one molecule and it can be used to calculate the molar free, f_m, volume of a solution [S6], by:

$$f_m = \left(V_m - R_m\right) \tag{2}$$

The values for the calculated molar refractions (from equation 1) and molar free volumes (from equation 2) of all the studied samples are listed in Tables S1 and S2 together with the molar volume calculated from density values. Figure S3 illustrates the molar free volumes for the neat ILs, $[C_2MIM][C_2SO_4]$ and $[C_2MIM][C_2SO_3]$, and their binary mixtures with $[NH_4][SCN]$ at a concentration of 0.3 in molar fraction of salt. It can be observed that the molar free volumes decrease with $[NH_4][SCN]$ concentration and increase as the temperature increases. In addition, the $[C_2MIM][C_2SO_4]$ ionic liquid shows higher molar free volume in the whole range of temperature, which means that it has more space available to accommodate $[NH_4][SCN]$ than $[C_2MIM][C_2SO_3]$. This is at least part of the answer for the higher solubility limit of the inorganic salts in $[C_2MIM][C_2SO_4]$ than in $[C_2MIM][C_2SO_3]$.

The analysis of the molar free volumes can be related with the solubility of different species in the mixtures of ionic liquid and inorganic salts, especially low molecular weight solutes that are gaseous at normal conditions. However, the mechanisms of solvation of some of these species, for example CO_2 [S7, S8] are controlled by the interactions and only to a minor extent by molar free volume effect [S9]. Therefore, refractive data can be useful to evaluate the importance of the dispersive molecular interactions and the size of the apolar domains (dominated by dispersive molecular interactions) in the pure ionic liquids or mixtures with ionic liquids [S6].

Table S2. Refractive index, n_D, molar volume, V_m, molar refraction, R_m, and free molar volume, f_m, for the binary system $[C_2MIM][C_2SO_4]$ (1) + $[NH_4][SCN]$ (2) at several temperatures.

x_2	n_D	V_m	R_m	f_m
		T = 298.15 K		
0	1.47875	191.0958	54.1652	136.9306
0.0235	1.47976	188.1278	53.4201	134.7077
0.1553	1.48477	171.8267	49.2259	122.6008
0.3025	1.48980	153.7266	44.4295	109.2972
0.4042	1.49582	141.0419	41.1887	99.8532
0.5205	1.50385	126.1104	37.3329	88.7776
0.5650	1.50987	120.2325	35.9516	84.2809
0.5997	1.51389	115.6491	34.8107	80.8384
		T = 303.15 K		
0	1.47775	191.6227	54.2176	137.4052
0.0235	1.47875	188.6468	53.4711	135.1757
0.1553	1.48277	172.2888	49.1845	123.1043
0.3025	1.48879	154.1176	44.4643	109.6534
0.4042	1.49381	141.4023	41.1518	100.2505
0.5205	1.50284	126.4337	37.3651	89.0686
0.5650	1.50887	120.5407	35.9841	84.5565
0.5997	1.51188	115.9646	34.7907	81.1740
		T = 308.15 K		
0	1.47674	192.1526	54.2691	137.8834
0.0235	1.47775	189.1686	53.5232	135.6454
0.1553	1.48177	172.7393	49.2259	123.5133
0.3025	1.48779	154.5106	44.5000	110.0106
0.4042	1.49181	141.7646	41.1152	100.6494
0.5205	1.50184	126.7586	37.3981	89.3605
0.5650	1.50686	120.8504	35.9563	84.8942
0.5997	1.51088	116.2530	34.8197	81.4333
		T = 313.15 K		
0	1.47474	192.6696	54.2197	138.4499
0.0235	1.47574	189.6778	53.4740	136.2038
0.1553	1.48076	173.1921	49.2666	123.9255
0.3025	1.48678	154.9056	44.5351	110.3706
0.4042	1.49080	142.1169	41.1454	100.9715
0.5205	1.50083	127.0746	37.4274	89.6471
0.5650	1.50586	121.1517	35.9858	85.1659
0.5997	1.50886	116.5429	34.7901	81.7528
		T = 318.15 K		
0	1.47373	193.2052	54.2713	138.9339
0.0235	1.47474	190.1898	53.5218	136.6679
0.1553	1.47875	173.6473	49.2195	124.4278
0.3025	1.48578	155.2898	44.5674	110.7225
0.4042	1.48980	142.4710	41.1764	101.2946
0.5205	1.49883	127.3815	37.3909	89.9907
0.5650	1.50485	121.4545	36.0149	85.4396
0.5997	1.50787	116.8342	34.8198	82.0144
		T = 323.15 K		
0	1.47273	193.7439	54.3241	139.4197
0.0235	1.47373	190.7045	53.5688	137.1357
0.1553	1.47675	174.1049	49.1729	124.9321
0.3025	1.48478	155.6888	44.6034	111.0854
0.4042	1.48879	142.8268	41.2068	101.6200
0.5205	1.49783	127.7006	37.4208	90.2798
0.5650	1.50385	121.7588	36.0446	85.7141
0.5997	1.50686	117.1269	34.8484	82.2785

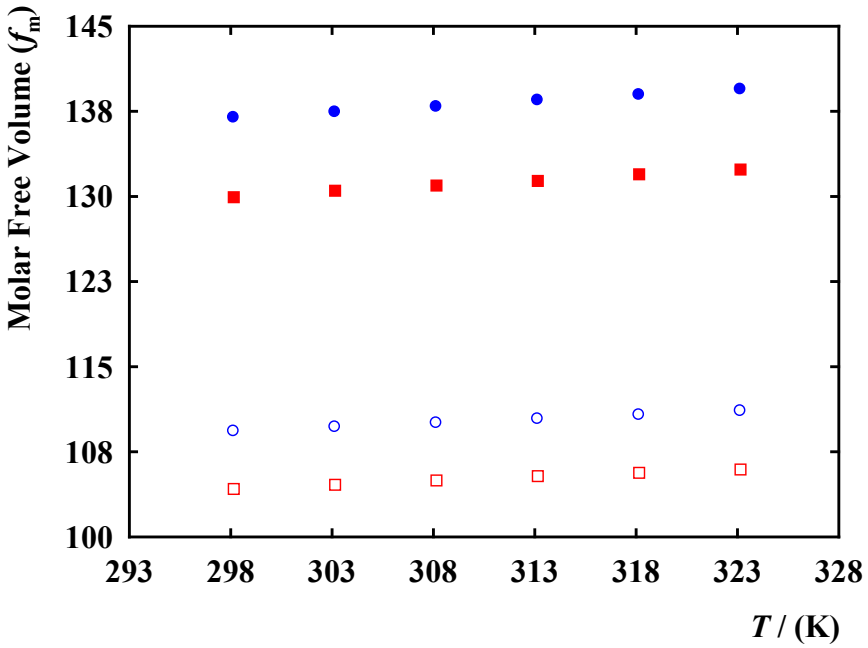

Figure S3. Molar Free Volume as a function of temperature for $[C_2MIM][C_2SO_4]$ (blue filled circle), $[C_2MIM][C_2SO_4] + x_{[NH4][SCN]}$=0.3 (blue empty circle), $[C_2MIM][C_2SO_3]$ (red filled square) and $[C_2MIM][C_2SO_3] + x_{[NH4][SCN]}$=0.3 (red empty square).

2.4. Thermogravimetric Analysis

The thermal decomposition temperatures as a function of inorganic salt concentration are listed in Table S3 and the onset temperature versus $[NH_4][SCN]$ concentration is plotted in Figure S4. The results for the binary mixtures indicate that the thermal decomposition temperatures decrease when the inorganic salt concentration increases. However, a deviation from this behaviour is observed for the binary mixture $[C_2MIM][C_2SO_4]$ + $[NH_4][SCN]$ in the onset temperatures at x $[NH_4][SCN]$ > 0.35. From this point, the onset temperatures stabilize with the addition of inorganic salt.

Table S3. Thermal decomposition temperatures for the binary system $[C_2MIM][C_2SO_3]$ or $[C_2MIM][C_2SO_4]$ (1) + $[NH_4][SCN]$ (2).

$[C_2MIM][C_2SO_3]$		$[C_2MIM][C_2SO_4]$	
x_2	T_{onset} (K)	x_2	T_{onset} (K)
0	626.20	0	621.29
0.0206	623.75	0.0235	620.93
0.1016	621.72	0.1553	605.10
0.2007	611.98	0.3025	573.80
0.3002	565.54	0.4042	529.17
1	462.97	0.5205	518.05

0.5650	517.84
0.5997	525.33
1	462.97

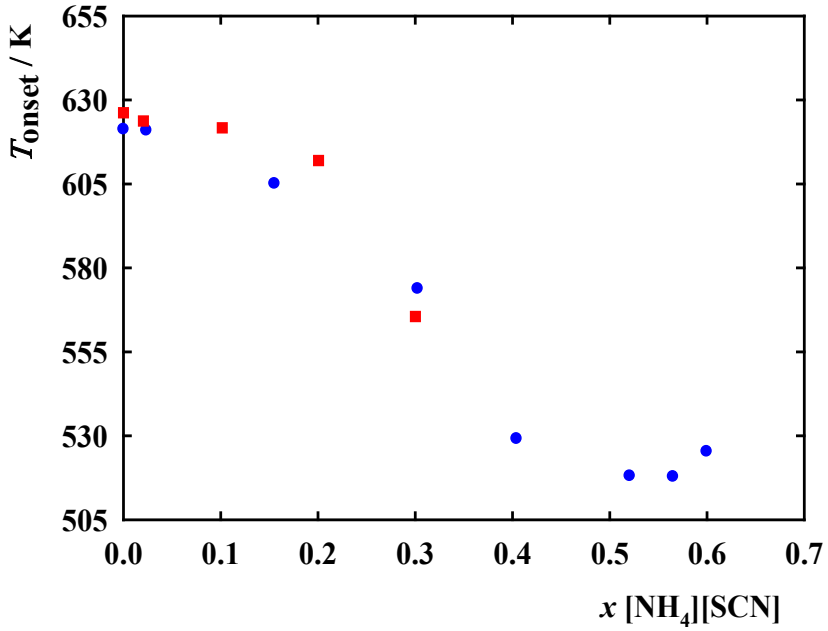

Figure S4. The onset temperature, T_{onset}, as a function of $[NH_4][SCN]$ concentration in the solubility range for the binary systems $[C_2MIM][C_2SO_4]$ (blue filled circle) or $[C_2MIM][C_2SO_3]$ (red filled square) + $[NH_4][SCN]$.

2.5. NMR Studies

Table S4. ^{1}H NMR and ^{13}C NMR chemical shifts (ppm) of $[C_2MIM][C_2SO_3]$ and the effect of $[NH_4][SCN]$ concentration upon the chemical shifts in DMSO–d_6 at 298.15 K.

	Molar fraction of $[NH_4][SCN]$									
Position	0	0.1332	0.2418	0.3384	0.3939	0	0.1332	0.2418	0.3384	0.3939
	^{1}H NMR					^{13}C NMR				
2	9.397	9.319	9.261	9.160	9.117	136.639	136.553	136.444	136.368	136.322
4	7.951	7.895	7.846	7.780	7.750	123.463	123.432	123.445	123.413	123.399
5	7.843	7.793	7.751	7.687	7.660	121.939	121.896	121.893	121.855	121.837
6	3.916	3.899	3.879	3.860	3.852	35.425	35.453	35.526	35.545	35.565
7	4.245	4.226	4.214	4.185	4.177	43.934	43.983	44.037	44.079	44.104
8	1.383	1.378	1.392	1.364	1.364	15.061	15.027	15.050	15.023	15.018
9	2.473	2.484	2.485	2.504	2.513	45.188	45.168	45.159	45.146	45.143
10	1.064	1.053	1.066	1.028	1.026	9.727	9.626	9.651	9.553	9.529
12	-	-	-	-	-	-	129.953	130.003	130.193	130.274

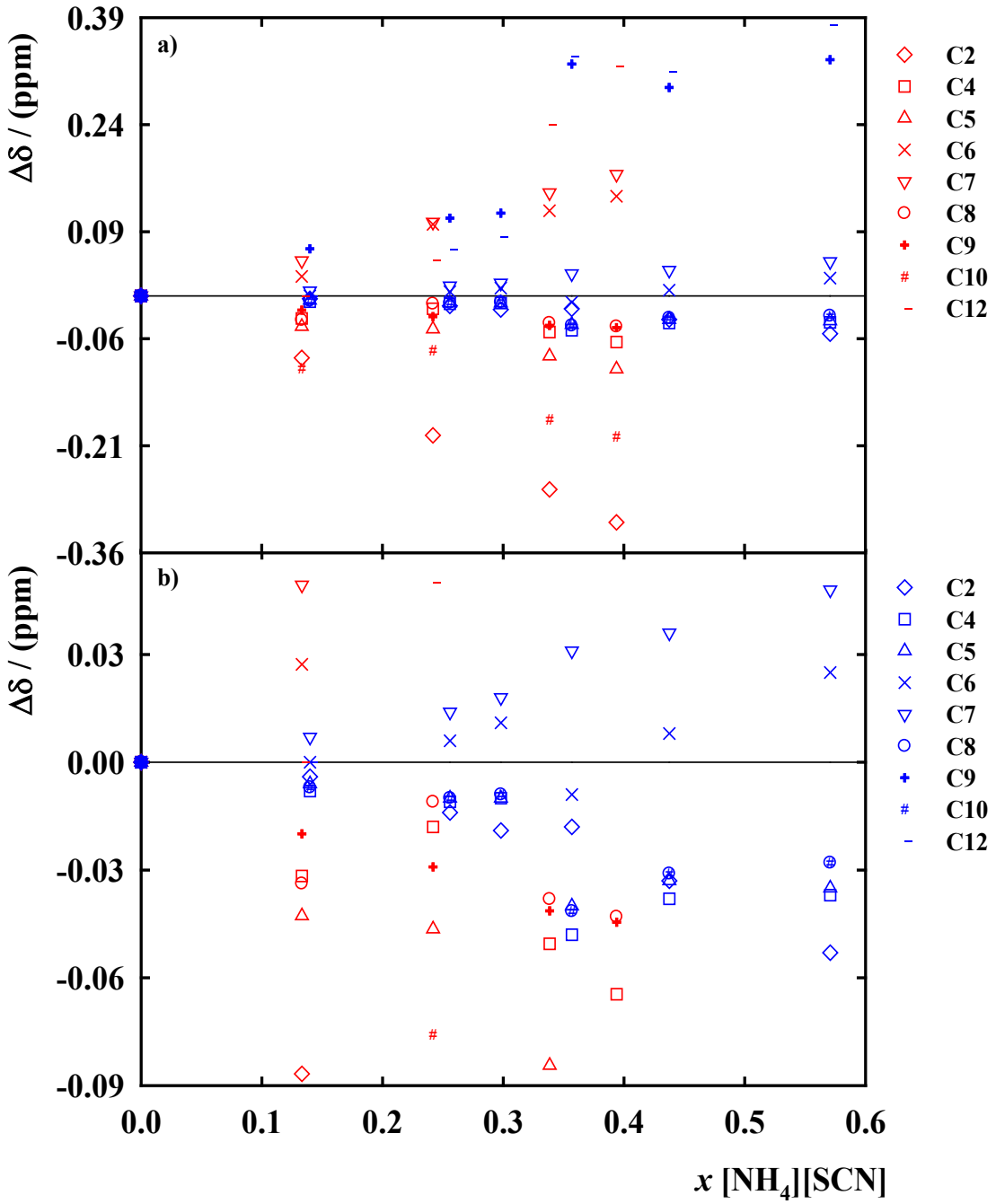

Figure S5. Trend of the chemical shift difference of carbons in ^{13}C NMR of $[C_2MIM][C_2SO_3]$ (red) and $[C_2MIM][C_2SO_4]$ [S1] (blue) with increasing $[NH_4][SCN]$ concentration ($\Delta\delta = \delta - \delta_{neat}$) (b is an enlarged image of a).

2.6. Raman Studies

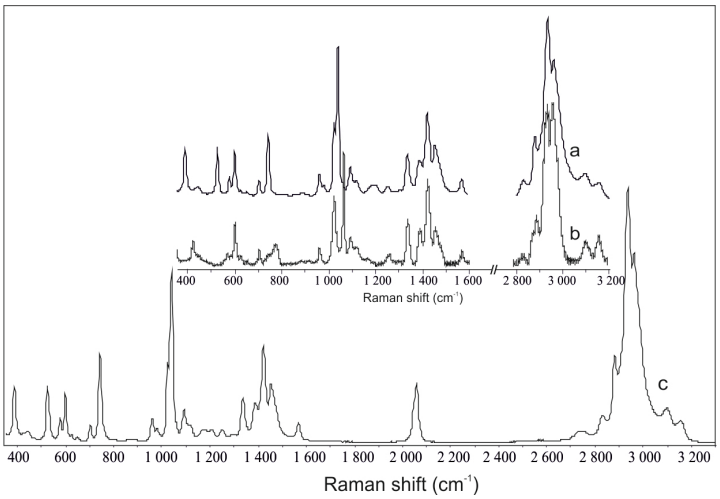

Figure S6. Raman spectra of a) $[C_2MIM][C_2SO_3]$, b) $[C_2MIM][C_2SO_4]$ and c) $[C_2MIM][C_2SO_3]$ + $[NH_4][SCN]$ ($x_{[NH4][SCN]}$ = 0.17). a) and c) were measured with 400 mW laser power and 1064 nm excitation; b) was recorded with 3 mW laser power, 60s accumulation time, and 413 nm excitation. Spectral intensities are normalized for clearer comparison.

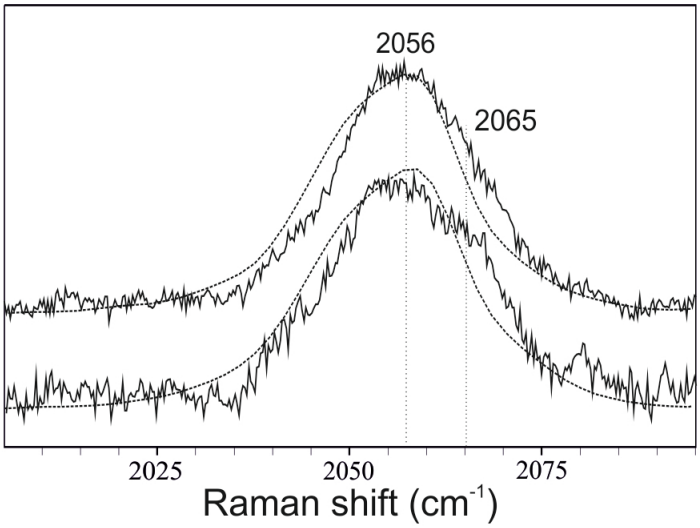

Figure S7. Raman spectra of $[C_2MIM][C_2SO_4]$ + $[NH_4][SCN]$ (solid lines) and $[C_2MIM][C_2SO_3]$ + $[NH_4][SCN]$ (dotted lines) binary mixtures, for $x_{[NH4][SCN]}$ = 0.17 (upper traces) and for $x_{[NH4][SCN]}$ = 0.25 (lower traces). Spectra of $[C_2MIM][C_2SO_4]$ +$[NH_4][SCN]$ were recorded with 3 mW laser power, 60s accumulation time, and 413 nm excitation. Spectra of the $[C_2MIM][C_2SO_3]$ + $[NH_4][SCN]$ mixtures were measured with 400 mW laser power and 1064 nm excitation. Spectral intensities were normalized to 1 for clearer comparison.

References

S1. A. B. Pereiro, J. M. M. Araújo, F. S. Oliveira, C. E. S. Bernardes, J. M. S. S. Esperança, J. N. C. Lopes, I. M. Marrucho and L. P. N. Rebelo, *Chem. Commun.*, 2012, **48**, 3656-3658.

S2. S. Tsuzuki, K. Hayamizu and S. Seki, *J. Phys. Chem. B*, 2010, **114**, 16329-16336.

S3. J. C. Lassegues, J. Grondin, C. Aupetit and P. Johansson, *J. Phys. Chem. A*, 2009, **113**, 305-314.

S4. M. J. Monteiro, F. F. C. Bazito, L. J. A. Siqueira, M. C. C. Ribeiro and R. M. Torresi, *J. Phys. Chem. B*, 2008, **112**, 2102-2109.

S5. M. R. Moldover, in *Vol. VI: Measurement of the Thermodynamic Properties of Single Phases*, eds. A. R. H. Goodwin, K. N. Marsh and W. A. Wakeham, Elsevier, 2003, pp. 435–451.

S6. M. Tariq, P. A. S. Forte, M. F. C. Gomes, J. N. C. Lopes and L. P. N. Rebelo, *J. Chem. Thermodyn.*, 2009, **41**, 790-798.

S7. C. Cadena, J. L. Anthony, J. K. Shah, T. I. Morrow, J. F. Brennecke and E. J. Maginn, *J. Am. Chem. Soc.*, 2004, **126**, 5300-5308.

S8. J. Deschamps, M. F. C. Gomes and A. A. H. Padua, *Chemphyschem*, 2004, **5**, 1049-1052.

S9. M. F. C. Gomes and A. A. H. Padua, *Pure Appl. Chem.*, 2005, **77**, 653-665.